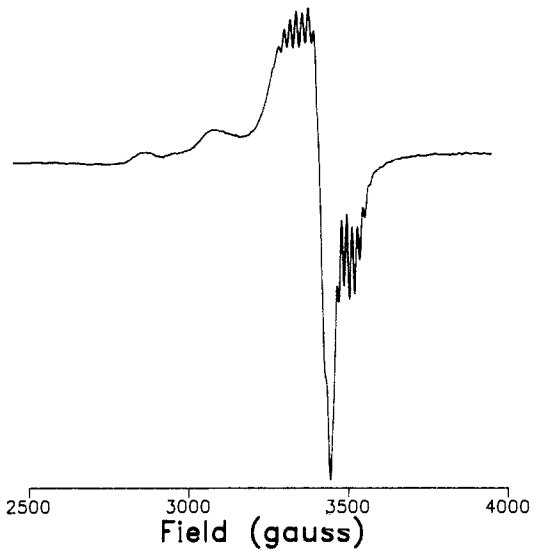

Figure 9. The ESR spectrum of a powdered sample of a $[Ni_{1-x}Cu_x(tatbp)]_3[ReO_4]_2 \cdot C_{10}H_7Cl$ solid solution. In this material 28% of the metal sites are occupied by Cu(II) ions.

structure likely is associated with trimers of the type [Ni(tatbp)-Cu(tatbp)-Ni(tatbp)]$^{2+}$. Observation of such structure is clear evidence that Cu-Cu spin exchange mediated by polarization of electrons in the nonbonding band of this semiconductor is not long range. In turn, this is consistent with the picture of strong Cu-Cu interactions within trimers but weak interactions between copper sites in different trimers.

Conclusions

$[Ni(tatbp)]_3[ReO_4]_2 \cdot C_{10}H_7Cl$ is a ligand-oxidized semiconductor with a band structure that can be derived by viewing the crystal packing as an extended array of weakly interacting supermolecules, each of which is composed of a trimer of three metallomacrocycles. The isostructural $[Cu(tatbp)]_3[ReO_4]_2 \cdot C_{10}H_7Cl$ exhibits strong Cu-Cu exchange coupling similar to that observed in Cu(L)I metallic conductors, and like the Cu(L)I metals this coupling is mediated by the π-electrons in the ligand-based band structure. However, metallic carrier electrons in the Cu(L)I systems move freely throughout the crystal lattice and mediate long-range Cu-Cu coupling, whereas ESR data on a $[Ni_{1-x}Cu_x(tatbp)]_3[ReO_4]_2 \cdot C_{10}H_7Cl$ solid solution indicate that the Cu-Cu coupling in this semiconductor is primarily limited to a trimer.

Acknowledgment. This work was supported by the National Science Foundation through Grant DMR-8818599 (B.M.H.) and through the Northwestern University Materials Research Center, Grant DMR-8821571.

Supplementary Material Available: Tables of anisotropic thermal parameters for Re and Cu and least-squares planes (2 pages); listing of $10|F_o|$ vs $10|F_c|$ (21 pages). Ordering information is given on any current masthead page.

Origin of the Strong Binding of Adenine to a Molecular Tweezer

James F. Blake and William L. Jorgensen*

Contribution from the Department of Chemistry, Purdue University, West Lafayette, Indiana 47907. *Received March 7, 1990*

Abstract: Monte Carlo statistical mechanics simulations and analyses of intrinsic interaction energies have been used to elucidate the observed strong binding of adenine derivatives to Zimmerman's molecular tweezer **3** in chloroform. Hydrogen bonding and π-stacking are found to contribute about equally to the remarkably strong interaction of the acid tweezer **6** and 9-methyladenine. The binding in chloroform is not enhanced by the existence of a naked binding cleft. Though 9-methyladenine easily wins the competition with chloroform for the binding site in **6**, the interaction between the ester tweezer **7** and 9-methyladenine is not adequate to displace the one or two chloroform molecules in the cleft. The absolute free energy of binding for the acid **6** and 9-methyladenine in chloroform was computed with the double-annihilation technique. The accord with the experimental data for acid **3** provides support for the validity of the theoretical analyses.

Specific interactions with nucleotide bases are under scrutiny in diverse areas including ribozyme chemistry,[1] formation of triple-helical DNA,[2] drug-DNA binding,[3] the chemistry of nucleic acid binding proteins,[4] and the association of chromosomes.[5] Much related activity is focusing on the development of synthetic hosts for the nucleoside bases. These studies are yielding valuable information on the factors that control molecular recognition in addition to providing a basis for the creation of novel, sequence-specific agents.[6] In fact, synthetic receptors have now been reported for all of the nucleoside bases.[7-10] Binding has been observed in chloroform solutions and features multiple hydrogen-bonding contacts and, sometimes, π-stacking interactions.

Hosts for adenine have been reported the most; it is an attractive target in view of the possibilities for both Watson-Crick and Hoogsteen hydrogen bonding. This is illustrated in Chart I where

Chart I

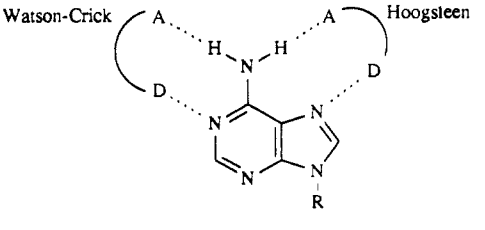

D and A refer to hydrogen-bond donor and acceptor sites. Elegant diversity is reflected in the structures of the adenine hosts, **1-4**,

* Address correspondence to this author at the Department of Chemistry, Yale University, New Haven, CT 06511.

(1) (a) Cech, T. R. *Science* **1987**, *236*, 1532. (b) Altman, S. *Adv. Enzymol.* **1989**, *62*, 1. (c) Piccirilli, J. A.; Krauch, T.; Moroney, S. E.; Benner, S. A. *Nature* **1990**, *343*, 33.

(2) (a) Moser, H. E.; Dervan, P. *Science* **1987**, *238*, 645. (b) Felsenfeld, G.; Davies, D. R.; Rich, A. *J. Am. Chem. Soc.* **1957**, *79*, 2023.

0002-7863/90/1512-7269$02.50/0

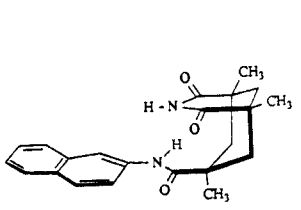

1

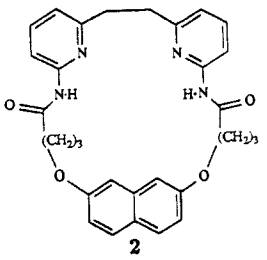

2

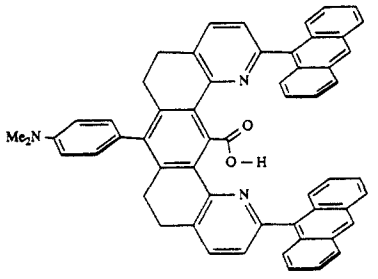

3

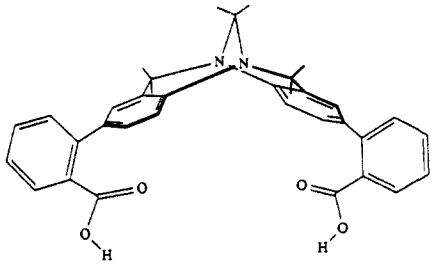

4

that come from the groups of Rebek, Hamilton, Zimmerman, and Wilcox, respectively.[7] Rebek's host **1** uses the imide edge for the donor–acceptor pair and also permits π-stacking with the naphthalene unit; a K_a of 220 M^{-1} is observed for this host with 9-ethyladenine (9-Et-A) in $CDCl_3$.[7a,11] Variation of the aryl unit was found to provide only a factor of ~2 enhancement of the K_a for each increment from phenyl to naphthyl to anthracyl. An elaborated version of the motif is provided by host **5**, which can simultaneously form the Watson–Crick and Hoogsteen pairings and yields a K_a of 11 000 M^{-1}.[7a] Four hydrogen bonds are also available through the amidopyridine fragments of Hamilton's macrocyclic host **2**. In conjunction with the π-stacking afforded by the naphthalene unit, a K_a of 3200 M^{-1} results for binding 9-butyladenine.[7b] Wilcox's host **4** provides another example of simultaneous formation of the four hydrogen bonds, though no π-stacking interaction is available. The benefit of the acid groups

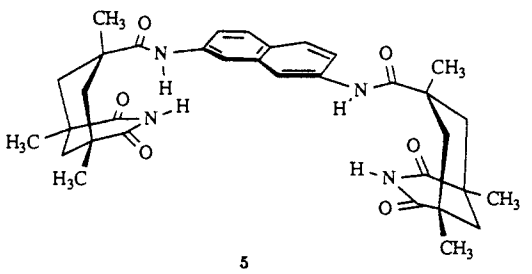

5

for hydrogen bonding is apparent in the impressive K_a of 45 000 M^{-1} for **4** with 9-Et-A in $CDCl_3$.[7d] By comparison, the binding potential for Zimmerman's "molecular tweezer" **3** might seem limited since the lone acid group can only yield two hydrogen bonds; however, the anthracyl plates are suited for two π-stacking interactions with the guest. In fact, the binding of 9-propyladenine to **3** in $CDCl_3$ is also impressive with a K_a of 25 000 M^{-1}.[7c] For reference, K_a's of 160 and 700 M^{-1} for complexation of 9-Et-A by butyric acid at 30 °C and by benzoic acid at 25 °C may be noted.[7d,12] Comparison with these results further emphasizes the remarkable binding achieved by host **3**. This led us to undertake computational studies directed at understanding the origin of the strong binding. In particular, the relative contributions from hydrogen bonding and π-stacking need to be clarified as well as the possibility that the binding cavity in **3** might be poorly solvated. Zimmerman and Wu also found that binding of 9-Pr-A by the methyl ester of **3** in $CDCl_3$ could not be detected by NMR, implying a K_a less than 10 M^{-1}.[7c,13] This result should be accommodated in the theoretical analysis as well.

Computational Approach

The plan of attack was to first demonstrate that the observed binding results can be reproduced through fluid simulations. If so, the underlying intermolecular interactions and structural results could then be confidently analyzed in depth.

For the purposes of the computations, a somewhat idealized version, **6**, of the tweezer has been used with 9-Me-A as the guest.

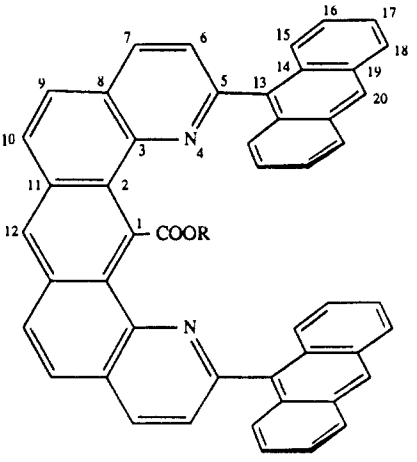

6 R = H

7 R = CH_3

In comparison to **3**, the dimethylanilinyl substituent has been removed and the pentacyclic spacer has been fully unsaturated. Neither modification is expected to strongly affect the binding results. However, the partially saturated rings cause twisting of the spacer in **3** such that the anthracene units are not as well aligned as in **6**.

The intended fluid simulations require complete specification of the molecular geometries, torsional potentials, and intermolecular potential functions corresponding to the solutes in chloroform.[14] These items will be addressed first, followed by a description of the Monte Carlo simulations.

Molecular Geometries. Since an X-ray structure is not available for **3**, the geometry of **6** was developed from AM1 calculations.[15]

(3) (a) Dugas, H. *Bioorganic Chemistry*; Springer-Verlag: New York, 1989; Chapter 3. (b) Hurley, L. H.; Warpehoski, M. *Chem. Res. Toxicol.* **1988**, *1*, 328.

(4) (a) Johnson, P. F.; McKnight, S. L. *Annu. Rev. Biochem.* **1989**, *58*, 799. (b) Normanly, J.; Abelson, J. *Annu. Rev. Biochem.* **1989**, *58*, 1029. (c) Rould, M. A.; Perona, J. J.; Soll, D.; Steitz, T. A. *Science* **1989**, *246*, 1135.

(5) (a) Sen, D.; Gilbert, W. *Nature* **1988**, *334*, 364. (b) Sundquist, W. I.; Klug, A. *Nature* **1989**, *342*, 825. (c) Williamson, J. R.; Raghuraman, M. K.; Cech, T. R. *Cell.* **1989**, *59*, 871.

(6) Rebek, J., Jr. *Science* **1987**, *235*, 1478.

(7) Adenine hosts: (a) Williams, K.; Askew, B.; Ballester, P.; Buhr, C.; Jeong, K. S.; Jones, S.; Rebek, J., Jr. *J. Am. Chem. Soc.* **1989**, *111*, 1090. (b) Goswami, S.; Hamilton, A. D.; Van Engen, D. *J. Am. Chem. Soc.* **1989**, *111*, 3425. (c) Zimmerman, S. C.; Wu, W. *J. Am. Chem. Soc.* **1989**, *111*, 8054. (d) Adrian, J. C., Jr.; Wilcox, C. S. *J. Am. Chem. Soc.* **1989**, *111*, 8055.

(8) Guanine hosts: (a) Hamilton, A. D.; Pant, N. *J. Chem. Soc., Chem. Commun.* **1988**, 765. (b) Rebek, J., Jr. *Chemtracts: Org. Chem.* **1989**, *2*, 337.

(9) Uracil or thymine hosts: (a) Hamilton, A. D.; Van Engen, D. *J. Am. Chem. Soc.* **1987**, *109*, 5035. (b) Muehldorf, A. V.; Van Engen, D.; Warner, J. C.; Hamilton, A. D. *J. Am. Chem. Soc.* **1988**, *110*, 6561.

(10) Cytosine hosts: Rebek, J., Jr.; Jeong, K. S. *J. Am. Chem. Soc.* **1988**, *110*, 3327.

(11) Unless stated otherwise, all K_a values are at 25 °C in chloroform.

(12) Lancelot, G. *J. Am. Chem. Soc.* **1977**, *99*, 7037.

(13) Zimmerman, S. C., personal communication.

(14) Jorgensen, W. L. *Acc. Chem. Res.* **1989**, *22*, 184.

In all aspects of this work, the pentacyclic and anthracene units were kept planar. AM1 optimizations were then carried out for the pentacyclic unit including the carboxylic acid and with hydrogens in place of the antracenes, and for an octacyclic molecule consisting of the pentacyclic piece and one anthracyl unit with hydrogens in place of the other anthracene and acid group. The results of these optimizations were merged to yield the geometrical parameters for **6**. An analogous process provided the geometry for the corresponding methyl ester **7**. And, the geometry of adenine was taken from results of an optimization via ab initio calculations with the 3-21G basis set and is fully planar.[16] A standard methyl group was appended to yield 9-Me-A.[17]

Intramolecular Potentials. Though the molecular tweezers are deliberately designed to be quite rigid, some torsional motion is possible, particularly for the acid group and for the hinges between the pentacyclic and anthracyl units. To include these in the simulations, the torsional potentials were examined with AM1 calculations. The fragments described above were used again. Optimizations were performed as a function of the dihedral angle for the bond between the pentacyclic unit and the carboxylic acid, and for the bond joining the pentacyclic and anthracyl units in the octacyclic molecule. In both cases an orthogonal arrangement is preferred. The AM1 results are well-represented by the single, 2-fold Fourier term in eq 1. For rotation of the acid group, the

$$V(\phi) = \frac{V_2}{2}[(1 - \cos(2\phi + \pi)] \qquad (1)$$

dihedral angle is CCCO and a V_2 of 22.1 kcal/mol is appropriate. For the biaryl torsion, the dihedral angle is CCCC and $V_2 = 11.7$ kcal/mol. In view of the high barriers, the sampling of the dihedral angles is expected to be confined within ca. ±30° of the minima at 90°.

Besides these torsional motions, the rotation of the acid hydrogen is also included. As described previously,[18] the Fourier series in eq 2 is appropriate with $V_1 = 4.98$ kcal/mol, and $V_2 =$

$$V(\phi) = \frac{V_1}{2}(1 + \cos\phi) + \frac{V_2}{2}(1 - \cos 2\phi) \qquad (2)$$

6.20 kcal/mol, where ϕ is the CCOH dihedral angle. The same torsional potential is also used for the methyl ester **7** where the dihedral angle is $CCOCH_3$.[18]

In the Monte Carlo calculations, the total intramolecular energy for the tweezers then consists of the sum of the four torsional potentials plus the nonbonded interactions that are not reflected in the origin of the torsional potentials. Specifically, one can view the tweezers as consisting of four domains: the pentacyclic piece, the two anthracyl units, and the acid or ester group. The interactions between the anthracyl units and pentacyclic piece and between the ester or acid group and pentacyclic piece are embodied in the torsional potentials. However, the interactions between the two anthracyl units and between each anthracyl unit and the acid or ester are not. Consequently, these nonbonded interactions are included using the standard Coulomb plus Lennard-Jones potentials described below.

Intermolecular Potential Functions. The intermolecular and the nonbonded intramolecular interactions are represented in the widely used Coulomb plus Lennard-Jones format of eq 3. Thus,

$$\Delta E_{ab} = \sum_i \sum_j \left(\frac{q_i q_j e^2}{r_{ij}} + \frac{A_{ij}}{r_{ij}^{12}} - \frac{C_{ij}}{r_{ij}^{6}} \right) \qquad (3)$$

the interaction energy between two molecules or two intramolecular units, a and b, is given by the double sum over all of the individual interactions between the interaction sites, i and j, in a and b.[18,19] The A and C parameters are related to Lennard-Jones σ's and ϵ's by $A_{ii} = 4\epsilon_i\sigma_i^{12}$ and $C_{ii} = 4\epsilon_i\sigma_i^{6}$, while the combining rules are $A_{ij} = (A_{ii}A_{jj})^{1/2}$ and $C_{ij} = (C_{ii}C_{jj})^{1/2}$.

Table I. OPLS Parameters for Molecular Tweezers **6** and **7**[a]

atom	q	σ	ϵ	atom	q	σ	ϵ
C2	0.000	3.550	0.070	H12	0.115	2.420	0.030
C3	0.230	3.750	0.110	C13	0.000	3.550	0.070
N4	−0.490	3.250	0.170	C14	0.000	3.550	0.070
C5	0.230	3.750	0.110	C15	−0.115	3.550	0.070
C6	−0.145	3.750	0.110	H15	0.115	2.420	0.030
H6	0.115	2.420	0.030	C16	−0.115	3.550	0.070
C7	−0.025	3.750	0.110	H16	0.115	2.420	0.030
H7	0.115	2.420	0.030	C17	−0.115	3.550	0.070
C8	−0.030	3.750	0.110	H17	0.115	2.420	0.030
C9	−0.115	3.550	0.070	C18	−0.115	3.550	0.070
H9	0.115	2.420	0.030	H18	0.115	2.420	0.030
C10	−0.115	3.550	0.070	C19	0.000	3.550	0.070
H10	0.115	2.420	0.030	C20	−0.115	3.550	0.070
C11	0.000	3.550	0.070	H20	0.115	2.420	0.030
C12	−0.115	3.550	0.070				
acid **6**				ester **7**			
C1	0.080	3.550	0.070	C1	0.050	3.550	0.070
C	0.550	3.750	0.105	C	0.550	3.750	0.105
O=	−0.500	2.960	0.210	O=	−0.450	2.960	0.210
O	−0.580	3.000	0.170	O	−0.400	3.000	0.170
H	0.450	0.000	0.000	CH_3	0.250	3.800	0.170

[a] Charge in electrons, σ in angstroms, ϵ in kilocalories per mole. Atom numbering is shown on structures **6** and **7** in the text.

The charges, q_i, and Lennard-Jones parameters used here have all been previously reported. Specifically, the OPLS four-site model was adopted for chloroform.[18] For aromatic rings, all-atom models are desirable.[20] Consequently, the all-atom potential functions devised recently for nucleoside bases were used here for adenine.[21] The potential functions were shown to give good results for gas-phase interaction energies and association constants for the bases in chloroform.[21] The parameters for the anthracene units in the hosts were taken from those for benzene with charges of zero on the fusion atoms,[20] while the parameters for the remainder of the hosts were adopted from those reported for benzene, pyridine, acetic acid, and methyl acetate.[18,20] All-atom representations were used for the hosts, except the methyl group in the methyl ester **7** was treated as a united atom centered on carbon in order to be consistent with the OPLS potential functions developed for methyl acetate.[18] A united-atom methyl group was also used at the 9-position in 9-Me-A.

The resultant parameters for the hosts are summarized in Table I. Although the Lennard-Jones parameters are highly transferable,[18-21] deviation of the partial charges for the hosts from constituent molecules is more questionable. The legitimacy of this approximation for the present systems was supported by the binding results and other observations discussed below in the section on gas-phase interaction energies.

Monte Carlo Simulations. Statistical mechanics calculations were carried out to compute (a) the relative free energies of binding of 9-Me-A to the acid and ester hosts and (b) the absolute free energy of binding of 9-Me-A and the acid **6**. The basic procedures for the calculations are now well-established.[14,22-24]

The former computation uses the thermodynamic cycle[22] in eq 4 and requires simulations in which the acid host is converted to the ester host in both the complexed and uncomplexed forms in

(15) Dewar, M. J. S.; Zoebisch, E. G.; Healy, E. F.; Stewart, J. P. *J. Am. Chem. Soc.* **1985**, *107*, 3902.
(16) Aida, M. *J. Comput. Chem.* **1988**, *9*, 362.
(17) The resultant geometries for **6**, **7**, and 9-Me-A are provided in Z-matrix form in the supplementary material.
(18) Jorgensen, W. L.; Briggs, J. M.; Contreras, M. L. *J. Phys. Chem.* **1990**, *94*, 1683.
(19) Jorgensen, W. L.; Tirado-Rives, J. *J. Am. Chem. Soc.* **1988**, *110*, 1657.
(20) Severance, D. L.; Jorgensen, W. L. *J. Am. Chem. Soc.* **1990**, *112*, 4768.
(21) Jorgensen, W. L.; Pranata, J. *J. Am. Chem. Soc.* **1990**, *112*, 2008. Pranata, J.; Wierschke, S. G.; Jorgensen, W. L. *J. Am. Chem. Soc.* Submitted.
(22) Tembe, B. L.; McCammon, J. A. *Comput. Chem.* **1984**, *8*, 281.
(23) Jorgensen, W. L.; Buckner, J. K.; Boudon, S.; Tirado-Rives, J. *J Chem. Phys.* **1988**, *89*, 3742.
(24) Beveridge, D. L.; DiCapua, F. M. *Annu. Rev. Biophys. Biophys. Chem.* **1989**, *18*, 431.

$$\begin{array}{ccc} \mathbf{6} + \text{9-Me-A} & \xrightarrow{\Delta G_1} & \mathbf{6}\cdot\text{9-MeA} \\ \downarrow \Delta G_3 & & \downarrow \Delta G_4 \\ \mathbf{7} + \text{9-Me-A} & \xrightarrow{\Delta G_2} & \mathbf{7}\cdot\text{9-MeA} \end{array} \quad (4)$$

chloroform. The relative free energy of binding is then obtained as $\Delta G_3 - \Delta G_4 = \Delta G_1 - \Delta G_2$. The free energy changes are computed from a series of Monte Carlo simulations by using statistical perturbation theory[25] in which the acid group is gradually converted to the ester.[14,24,26] For the complexed form, two series of simulations were actually run, one starting with the **6**·9-Me-A complex hydrogen bonded in the Watson–Crick orientation, and the other in the Hoogsteen mode. All simulations for the complexes included the host, 9-Me-A, and 250 chloroform molecules in a cubic box with an edge length of ca. 33 Å. The interconversion of the uncomplexed hosts was also performed in a cubic box with 250 chloroform molecules. All simulations followed standard procedures including use of periodic boundary conditions, Metropolis and preferential sampling, and the isothermal isobaric ensemble at 25 °C and 1 atm.[24,26] The solvent–solvent interactions were spherically truncated at a C–C separation of 11 Å with quadratic feathering over the last 0.5 Å. A solute–solvent interaction was included with the same feathering if the distance between the carbon of chloroform and essentially any non-hydrogen atom in the solute was less than 11 Å. We have found that the feathering reduces fluctuations in the free energy calculations in comparison to abrupt truncation. A total of five simulations was used for each interconversion of the acid and ester hosts. This gave 10 incremental free energy changes by perturbing in both directions, which has been termed "double-wide sampling".[26] Each simulation consisted of 0.8×10^6 configurations of equilibrium followed by 2.0×10^6 configurations of averaging. The solutes moved completely independently and the sampling for the hosts included variations of the four dihedral angles discussed above.

Computation of the absolute free energy of binding, ΔG_b, is more arduous. The most efficient current procedure can be called "double annihilation". It entails two series of simulations in which the guest is made to disappear in the solvent in both the complexed and uncomplexed forms.[23] The thermodynamic relationship readily emerges from eq 5; i.e., $\Delta G_b = \Delta G_u - \Delta G_c$. For the removal

$$\begin{array}{lll} \mathbf{6} \rightarrow \mathbf{6}\cdot\text{9-Me-A} & -\Delta G_c \\ \text{9-Me-A} \rightarrow 0 & \Delta G_u \\ \hline \mathbf{6} + \text{9-Me-A} \rightarrow \mathbf{6}\cdot\text{9-Me-A} & \Delta G_b \end{array} \quad (5)$$

of a solute as large as 9-Me-A, numerous simulations are required to slowly shrink it; otherwise, the fluctuations in the computed incremental free energy changes are large and the results become unacceptably imprecise. We ended up using 19 and 22 simulations for computing ΔG_c and ΔG_u, respectively. The details of the simulations were identical with those described for the interconversions of **6** and **7** The number of simulations that were required was arrived at partly from experience[23,27] and from observation of the present calculations. During the calculations, separate averages for the free energy changes are computed for each block of $(1-2) \times 10^5$ configurations. If the resultant standard deviation for the average free energy change exceeded ca. 0.1 kcal/mol, the increment for the perturbation variable, λ,[22,26] was reduced and a new simulation with smaller $\Delta\lambda$ was executed. Some free energy increments were also checked by computing them forwards and backwards. The entire mutation of 9-Me-A to nothing was run in both directions. The outcome of these calculations and some other technical points are covered under Results and Discussion.

The statistical mechanics simulations were carried out with the BOSS program, version 2.7, on Silicon Graphics 4D and Sun workstations in our laboratory. The results reported below for optimizations of gas-phase complexes were also obtained with this program. Very low temperature simulations are performed such that essentially the only Monte Carlo moves that are accepted lower the total energy. Alternative starting geometries for the complexes are conveniently generated by high-temperature Monte Carlo runs. The procedure yielded identical results for a variety of test cases that were also optimized by alternative methods such as grid search and simplex. However, there are clear benefits in convenience for using the BOSS program for both types of calculations.

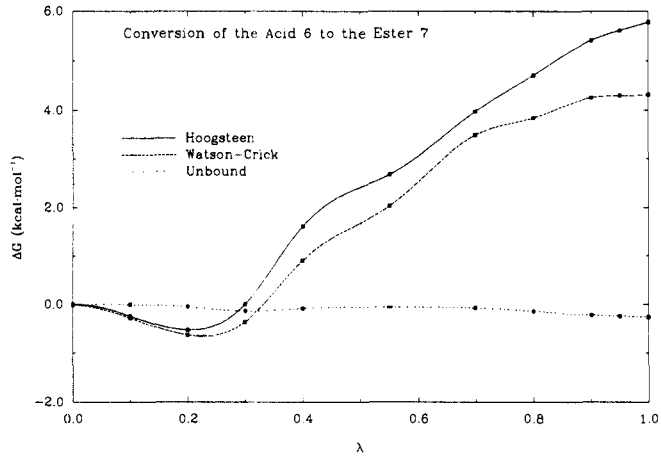

Figure 1. Computed change in the free energy for the interconversion of hosts **6** and **7** both complexed with 9-Me-A and uncomplexed in chloroform at 25 °C.

Results and Discussion

Relative Binding for the Acid and Ester Tweezers. The courses of the free energy calculations for the three mutations of the acid **6** to the ester **7** are summarized in Figure 1. The cumulative free energy changes are shown for going from the acid at $\lambda = 0$ to the ester at $\lambda = 1$. The smoothness of the curves is accompanied by small standard deviations for the overall free energy changes. For the unbound hosts, it is found that ΔG_3 in eq 4 is -0.27 ± 0.12 kcal/mol. This reflects both the difference in solvation and intramolecular energy for the tweezers. Due to the additional nonbonded interactions with the methyl group, the latter term actually favors the ester by 2.2 kcal/mol according to the simulations. So, the acid tweezer is, in fact, better solvated than the ester by ~2 kcal/mol. This contrasts with our previous study of the mutation of acetic acid to methyl acetate, which yielded a lower free energy of solvation for the ester by 0.49 ± 0.09 kcal/mol.[18]

For the complexes with 9-Me-A, mutation of the acid to ester is significantly destabilizing in accord with reduction in the intersolute hydrogen bonding. When the complex starts in the Watson–Crick orientation, ΔG_4 in eq 4 is computed to be 4.33 ± 0.29 kcal/mol, while 5.79 ± 0.30 kcal/mol is obtained in the Hoogsteen geometry. During these simulations interconversion of the Watson–Crick and Hoogsteen forms did not occur; i.e., the carbonyl oxygen of the acid or ester group remained hydrogen bonded to the appropriate hydrogen on the nitrogen at C6 of 9-Me-A.

Combination of the results for ΔG_3 and ΔG_4 yields preferences of 4.6 ± 0.3 and 6.1 ± 0.3 kcal/mol for binding 9-Me-A to the acid tweezer over the ester in the Watson–Crick and Hoogsteen forms. These values translate to K_a ratios of 2300 and 27 000, respectively, plus or minus ~50%. The experimental K_a for 9-Pr-A with **3** is $25\,000 \pm 6000$ M^{-1} and for 9-Pr-A with the methyl ester of **3** is <10 M^{-1}.[7c,13] Assuming that the K_a for the methyl ester of **3** is ~1 M^{-1}, the present theoretical results appear reasonable. However, the lingering uncertainty led us to computation of the absolute free energy of binding.

The present theoretical findings do not establish the preference for the acid tweezer binding in the Watson–Crick or Hoogsten modes. Though this could be done by mutating from Watson–Crick to Hoogsteen, some data are already available that suggest

(25) Zwanzig, R. W. *J. Chem. Phys.* **1954**, *22*, 1420.
(26) Jorgensen, W. L.; Ravimohan, C. *J. Chem. Phys.* **1985**, *83*, 3050.
(27) Jorgensen, W. L.; Blake, J. F.; Buckner, J. K. *Chem. Phys.* **1989**, *129*, 193.

Table II. Computed Free Energy Changes for the Creation of 9-Methyladenine in Chloroform[a]

λ_i	λ_j	ΔG, i to j	σ	ΔG, j to i	σ
0.000	0.075	−0.096	0.005	0.155	0.009
0.075	0.150	−0.315	0.018	0.490	0.030
0.150	0.200	−0.355	0.024	0.508	0.023
0.200	0.250	−0.514	0.017	0.608	0.026
0.250	0.300	−0.533	0.024	0.700	0.038
0.300	0.350	−0.534	0.040	0.741	0.037
0.350	0.400	−0.598	0.033	0.683	0.073
0.400	0.450	−0.577	0.039	0.771	0.045
0.450	0.500	−0.626	0.048	0.860	0.061
0.500	0.550	−0.643	0.070	0.799	0.069
0.550	0.600	−0.630	0.077	0.790	0.056
0.600	0.650	−0.627	0.113	0.624	0.105
0.650	0.700	−0.599	0.066	0.681	0.154
0.700	0.750	−0.793	0.098	0.754	0.098
0.750	0.800	−0.702	0.059	0.892	0.064
0.800	0.850	−0.658	0.117	0.946	0.071
0.850	0.900	−0.875	0.082	1.067	0.074
0.900	0.925	−0.473	0.047	0.462	0.045
0.925	0.950	−0.485	0.048	0.415	0.068
0.950	0.975	−0.522	0.058	0.432	0.052
0.975	1.000	−0.439	0.048	0.493	0.047
total		−11.594	0.283	13.871	0.307

[a] Free energies and standard deviations in kilocalories per mole.

that the Hoogsteen geometry is preferred. As presented below, optimizations of the gas-phase complexes for **6** and 9-Me-A favor the Hoogsteen orientation by 1.2 kcal/mol. Furthermore, the binding of **3** and 6-*N*-methyl-9-ethyladenine is observed to be essentially the same as for 9-Pr-A.[13] Since the *N*-methyl group resides primarily on the N1 side,[28] the loss of the potential Watson–Crick interaction does not reduce the binding.

Absolute Free Energy of Binding for the Acid Tweezer. Under the circumstances, it was decided to execute the disappearance of the 9-Me-A starting from the Hoogsteen form of the complex with acid **6**. First, however, the mutation of 9-Me-A to nothing was studied as the mutation variable λ went from 1 to 0. Not only were the charges and Lennard-Jones parameters linearly scaled with λ, the bond lengths were as well. Two complete series of 11 simulations each were run with double-wide sampling to give the free energy change for each increment in both directions, $\lambda_i \rightarrow \lambda_j$ and $\lambda_j \rightarrow \lambda_i$. The results are tabulated in Table II. It is seen that the spacing in Δλ was not uniform; rather, smaller increments are used near the fully formed solute at λ = 1. It may also be noted that the standard deviations, σ, computed from the block subaverages average ~0.05 kcal/mol and are almost all under 0.1 kcal/mol. In addition, there is generally good accord in the magnitudes of the free energy changes for $\lambda_i \rightarrow \lambda_j$ and $\lambda_j \rightarrow \lambda_i$ with the signs of the numbers opposite, of course. Closer inspection reveals a tendency for the magnitudes of the free energy changes to be slightly smaller for the perturbations that increase the size of the solute ($\lambda_i \rightarrow \lambda_j$) than for those that decrease it ($\lambda_j \rightarrow \lambda_i$). As shown in Figure 2, the effect accumulates over the 21 increments to cause significant divergence in the overall free energy changes for the $\lambda_i \rightarrow \lambda_j$ and $\lambda_j \rightarrow \lambda_i$ series. The computed total ΔG's predict free energies of solvation in chloroform of −11.6 ± 0.3 and −13.9 ± 0.3 kcal/mol, respectively, for the two series. It is important to note that the average of these values, −12.7 kcal/mol, is in good accord with the results of −12.6 ± 0.3 and −12.9 ± 0.3 that are obtained from the two series of 11 simulations with the double-wide sampling. In these cases, half of the increments are for $\lambda_i \rightarrow \lambda_j$ and half are for $\lambda_j \rightarrow \lambda_i$. Thus, the apparent systematic errors cancel.

The origin of the systematic error can be rationalized as follows. The computed free energy increments are likely all too positive by small amounts; i.e., for the creation steps, $\lambda_i \rightarrow \lambda_j$, the computed increment is $-x + c$ and for the annihilation steps, $\lambda_j \rightarrow \lambda_i$, it is

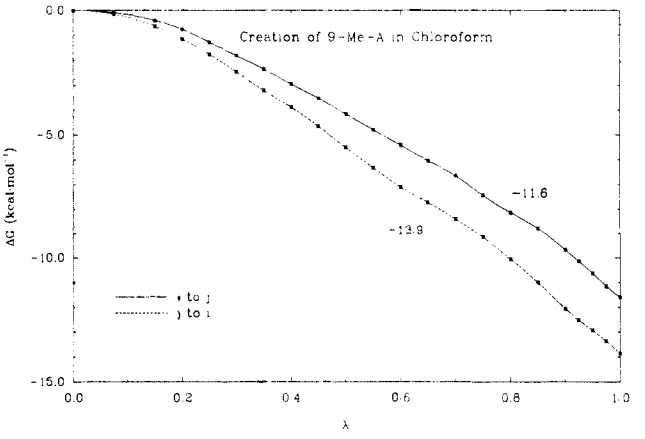

Figure 2. Computed change in the free energy for the creation (or disappearance) of 9-Me-A in chloroform. λ = 1 corresponds to the fully formed solute.

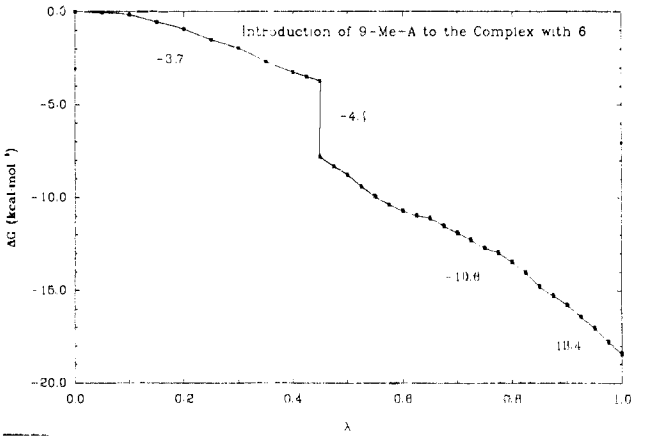

Figure 3. Computed change in the free energy for introduction of 9-Me-A to the complex with **6**. The dashed line represents the free energy required to remove the remaining charge from 9-Me-A at λ = 0.45. λ = 1 corresponds to the Hoogsteen hydrogen-bonding orientation of 9-Me-A with **6**.

$x + c$ where x is the true free energy change and c is the systematic error. The average for the increment $\lambda_i \rightarrow \lambda_j$ using both perturbations is, however, correct: $[(-x + c) - (x + c)]/2 = -x$. This averaging is also achieved by the double-wide sampling. The reason that the computed free energy changes are all too positve is that the perturbations are too big. Formally, the solvent configurations for the reference solute do not provide appropriate enough configurations for the perturbed solutes. Or, more graphically, on the expansion steps, the perturbed solute smacks into the solvent too much, while it pulls away from the solvent too much on the contraction steps. In summary, the results for $\lambda_i \rightarrow \lambda_j$ and $\lambda_j \rightarrow \lambda_i$ should be identical with opposite sign. However, even with the use of 21 increments for the present mutation, systematic errors are evident. Though they could presumably be eliminated by using even smaller Δλ's, in the absence of this, it is clearly advisable to use double-wide sampling and accumulate the incremental free energy changes from mutations that are half in one direction and half in the other.

The recommended procedure is the natural one with the BOSS program since it always performs the double-wide sampling. The procedure was followed in the subsequent series of simulations that removed 9-Me-A from the complex with the acid tweezer **6**. In this case 19 simulations were used to give 38 incremental free energy changes. The progress of the calculations as a function of λ is recorded in Figure 3. Starting at λ = 1 with the fully formed 9-Me-A in the Hoogsteen orientation, the computations proceeded normally until λ reached ~0.45. The simulation at this point then showed an anomalously low intersolute energy accompanied by severe fluctuations in the free energy increments. The problem was found to arise as follows. The shrunken guest has partial charges and Lennard-Jones σ's that have been reduced

(28) (a) Dodin, G.; Dreyfus, M.; Dubois, J.-E. *J. Chem. Soc., Perkin Trans. 2* **1979**, 439. (b) Rebek, J., Jr.; Williams, K.; Parris, K.; Ballester, P.; Jeong, K.-S. *Angew. Chem., Int. Ed. Engl.* **1987**, *26*, 1244.

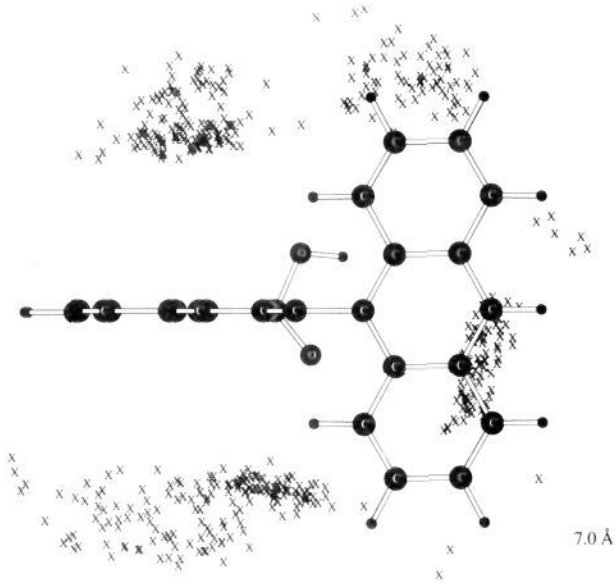

Figure 4. Graphical analysis of acid host **6** (top view) in chloroform. X's correspond to the location of a chloroform carbon that is within 7 Å of the carbonyl carbon. A total of 80 configurations were used in the analysis.

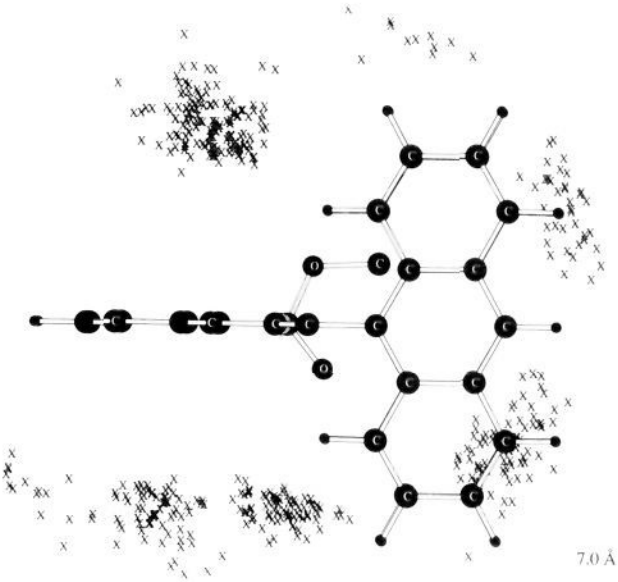

Figure 5. Graphical analysis of ester host **7** (top view) in chloroform. X's correspond to the location of a chloroform carbon that is within 7 Å of the carbonyl carbon. A total of 80 configurations were used in the analysis.

by about half at this point. The effect on the $1/r^{12}$ short-range repulsions is much greater than on the Coulombic interactions owing to the dependence of the former on $\sigma_{AA}^6\sigma_{BB}^6$. The reduced repulsion allows a partially negatively charged atom in the shrunken 9-Me-A to become almost coincident with the position of the acid hydrogen of **6**. This leads to the very low energy and unacceptable noise in the free energy perturbations. Consequently, a pause was taken at $\lambda = 0.45$ and the remaining charge on the guest's atoms was stripped away without changing the σ's and ϵ's. The charge removal was readily achieved in three simulations giving six incremental free energy changes. The free energy rose by 4.09 ± 0.14 kcal/mol during this segment as noted in Figure 3. The reduction in the σ's, ϵ's, and bond lengths then proceeded until the guest vanished at $\lambda = 0$. The charge stripping was not necessary in the simulations that removed the 9-Me-A by itself in chloroform presumably due to the absence of interaction sites in the solute's environment that have zero for σ and ϵ like the acid hyrdogen (Table I).

Overall, the computed free energy change for removal of the 9-Me-A from the complex with **6**, ΔG_c in eq 5, is 18.4 ± 0.4 kcal/mol. Combination with the computed value of ΔG_u, 12.7 ± 0.4, gives an absolute free energy of binding, ΔG_b, of −5.7 ± 0.6 kcal/mol. The experimental result from the K_a of 25 000 ± 6000 M^{-1} for 9-Pr-A binding with **3** is −6.0 ± 0.1 kcal/mol. Even though **3** and **6** are not identical, the level of accord is still gratifying.[34] It supports the appropriateness of the potential functions and provides a basis for faith in the following analyses of the intermolecular interactions. The present results are also a promising sign for further application of the "double-annihilation" procedure, which has only been used twice up to now.[23,29]

Solvation of the Binding Cleft. Before considering the intermolecular interactions in detail, one issue that is easily addressed from the fluid simulations is the solvation of the binding cleft in the acid and ester tweezers. Specifically, if the cleft was poorly solvated, a vacuum-like environment would be created that could lead to very strong binding of an appropriate guest.[30] Monte Carlo simulations were run for the acid **6** and ester **7** alone in chloroform. A total of 80 configurations were saved for each system spaced evenly during the 2×10^6 configurations of averaging. The plots shown in Figures 4 and 5 were then made where an X indicates

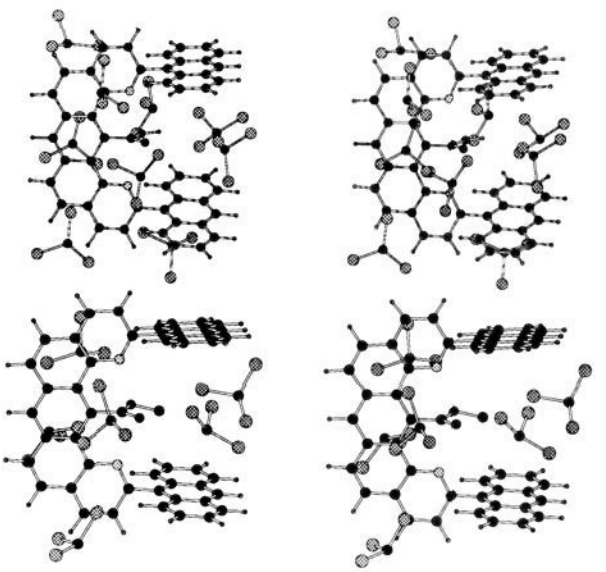

Figure 6. Stereoplots from the last configurations in the simulations of the uncomplexed hosts **6** (top) and **7** (bottom). Only chloroform molecules with any atom within 7 Å of the carbonyl carbon of the host are shown.

the location of a chloroform carbon in one of the 80 configurations that is within 7 Å of the carbonyl carbon of the acid or ester. The views in the plots are from above looking down upon the coincident anthracene plates. For the acid tweezer, Figure 4 indicates that there is always one chloroform molecule well-buried in the cleft with its carbon roughly in line with the outer carbons of the anthracene units. Labeling the number of the chloroform establishes that the cluster of X's is only due to one chloroform molecule. There is also a chloroform molecule on either side of the pentacyclic fragment that is solvating the oxygen atoms of the acid.

The local solvation of the ester **7** is shown equivalently in Figure 5. Again, a chloroform molecule is between the anthracene plates in a position shifted down a little in the figure compared to the case for the acid. There is also a second chloroform molecule at the edge of the cleft that may be interacting favorably with the methyl group of the ester. In addition, chloroform molecules are again found on both sides of the pentacyclic fragment in positions

(29) Sneddon, S. F.; Tobias, D. J.; Brooks, C. L., III *J. Mol. Biol.* **1989**, *209*, 817.
(30) Chapman, K. T.; Still, W. C. *J. Am. Chem. Soc.* **1989**, *111*, 3075.

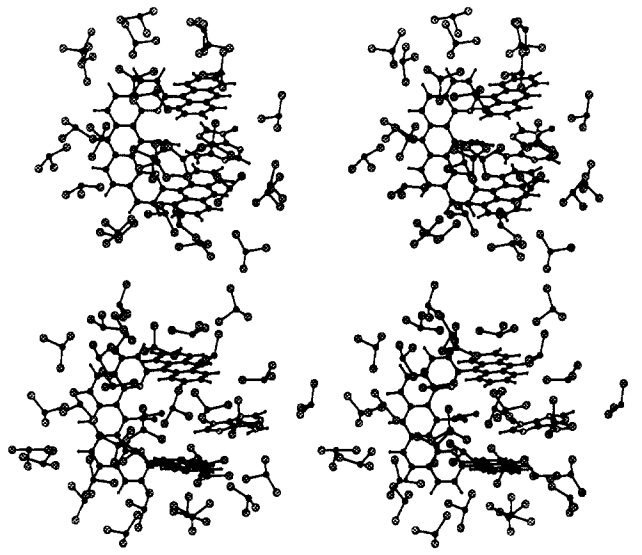

Figure 7. Stereoplots from the last configurations in the simulations of the complexes between the acid (top) and ester (bottom) hosts, **6** and **7**, and 9-Me-A. The complexes were initially in the Hoogsteen orientation. Only chloroform molecules with any atom within 3.5 Å of any atom in the host or guest are shown.

consistent with solvation of the ester oxygens.

These descriptions are supported by stereoplots of individual configurations from the simulations. Figure 6 shows the chloroform molecules with any atom within 7 Å of the carbonyl carbons for the acid and ester tweezers in the last configuration from the Monte Carlo simulations of the uncomplexed hosts. Note that the hydrogen of chloroform is implicit in the OPLS four-site model.[18] In both cases, one chloroform molecule is well inside the cleft and another is between the outer edges of the anthracenes, consistent with Figures 4 and 5. For comparison, the last configurations from the simulations of the complexes with 9-Me-A are illustrated in Figure 7. All chloroform molecules with any atom within 3.5 Å of any atom in the host or guest are now shown and the initial orientation was for Hoogsteen binding. The complex with the acid shows the two-point hydrogen bonding with the guest fully occupying the binding cleft. However, for the ester, the host–guest hydrogen bonding has been lost, the guest has moved significantly out of the cleft, and a chloroform molecule has entered the cleft in the rear of the picture.

Thus, naked clefts are not found and any guest must compete with the chloroform solvent for binding to the tweezers. In systematic studies of a series of molecular tweezers with a cleft geometrically similar to that of **3**, Zimmerman et al. also obtained data that indicate the clefts are solvated in chloroform.[31]

Optimizations of Gas-Phase Complexes. At this point, it is appropriate to analyze the intrinsic gas-phase interactions for insights on the strong binding for the acid, the negligible binding for the ester, and the relative importance of hydrogen bonding and π-stacking.

For reference, Figure 8 illustrates the results of optimizations for 9-Me-A with acetic acid and methyl acetate using the OPLS potential functions. In all cases the reported net interaction energies come from taking the difference of the optimized energies for the complex and the individual molecules. The Watson–Crick orientation is preferred by 0.8 kcal/mol for acetic acid, while the Watson–Crick and Hoogsteen alternatives are essentially isoenergetic for methyl acetate. Reduction to one hydrogen bond makes the optimal interaction ~6 kcal/mol weaker for the ester.

Figures 9 and 10 contain the corresponding results for 9-Me-A with the acid **6** and ester **7**. There is a dramatic enhancement of binding for **6** compared to acetic acid, which will be shown to arise predominantly from the π-stacking. There is also a reversal such that the Hoogsteen form is now preferred by 1.2 kcal/mol; this orientation allows greater contact between the aromatic surfaces as seen in Figure 9. The optimal interaction energy of −23.9 kcal/mol represents an enhancement of 12 kcal/mol over binding acetic acid. The binding of 9-Me-A to the ester **7** is much weaker. The second hydrogen bond is lost and the methyl group pushes the guest farther out of the cleft, which reduces the potential for π-stacking. There is still no significant preference for the Watson–Crick or Hoogsteen orientations. However, the optimal interaction has been enhanced by 8 kcal/mol to −14.3 kcal/mol in comparison to binding with methyl acetate.

The far stronger gas-phase binding for the acid **6** than ester **7** is much more than enough to account for the observed and computed K_a ratios. However, a dilemma arises here that also illustrates the limited utility of just considering gas-phase interaction energies to illuminate condensed-phase binding. As mentioned in the introduction, butyric acid is observed in chloroform to have a K_a of 160 M^{-1} with 9-Et-A.[12] The optimal gas-phase interaction for this pair must be near the −11.8 kcal/mol for acetic acid with 9-Me-A in Figure 8. So, why should the ester of **3** with an optimal interaction of ca. −14.3 kcal/mol based on Figure 10 reveal no binding with 9-Pr-A?[7c] The answer is that the tweezers are also great hosts for the solvent, chloroform. This is documented in Figure 11. The optimized complexes of **6** and **7** with a chloroform molecule give interaction energies of −12.4 and −10.6 kcal/mol. The chloroform molecule is buried in the cleft with its carbon atom positioned in a manner consistent with the results in Figures 4 and 5. For comparison, the optimal interaction energies for acetic acid and methyl acetate with chloroform are computed to be −3.6 and −3.7 kcal/mol. Thus, chloroform also enjoys highly favorable interactions with the anthracene units. Overall, chloroform cannot compete with the binding of 9-Me-A to the acid tweezer in view of the much stronger (11.5 kcal/mol) optimal interaction for the 9-Me-A. However, the difference is only 3.7 kcal/mol for the optimal interactions of the ester tweezer **7** with 9-Me-A and a chloroform molecule, and there are two chloroform molecules in proximity to the cavity (Figure 5). Consequently, 9-Me-A does not compete well with chloroform for binding to the ester tweezer even though the optimal gas-phase interaction for **7** with 9-Me-A is stronger than for some systems such as butyric acid with 9-Et-A that do show binding.

The importance of the π-stacking in these systems is readily demonstrated by replacing the anthracene plates with hydrogens. The potential functions are the same (Table I) except the capping hydrogens and adjacent carbons have been assigned charges of 0.115. The optimal structures obtained upon successive deletion of the anthracene fragments are shown in Figure 12 for binding 9-Me-A and the acids. With one anthracene unit, the Hoogsteen mode is still preferred by 0.4 kcal/mol with an optimal interaction energy of −19.7 kcal/mol. Deletion of the second anthracene unit weakens the optimal interaction to −13.4 kcal/mol and the Hoogsteen geometry is favored by only 0.2 kcal/mol. Thus, in going from zero to one to two anthracene units, the optimal interaction energy is enhanced by 6.3 and then 4.2 kcal/mol. The π-stacking can be assigned 10.5/23.9 or 44% of the total interaction energy for **6** with 9-Me-A. The remainder comes primarily from the hydrogen bonding to the pentacyclic acid fragment.

As mentioned above, some study of the sensitivity of the optimization results to the choice of partial charges for the acid host was performed. The Lennard-Jones parameters in Table I were used in all cases. First, the sensitivity to the charges on the anthracene fragments was explored. OPLS charges were used for the COOH group and then the rest of the charges were simply taken from the results of the AM1 population analysis for the octacyclic molecule with adjustment for C1 to preserve neutrality. Optimizations with 9-Me-A lead to geometries of the complexes nearly identical with those in Figure 9. And, the interaction energies are also essentially identical with those in Figure 9 at −22.6 and −23.6 kcal/mol for the Watson–Crick and Hoogsteen forms with the AM1 charges. In another test, the OPLS charges were used, except that the charges for all of the atoms in the anthracene units were set to zero. The Watson–Crick and

(31) Zimmerman, S. C.; Mrksich, M.; Baloga, M. *J. Am. Chem. Soc.* **1989**, *111*, 8528.

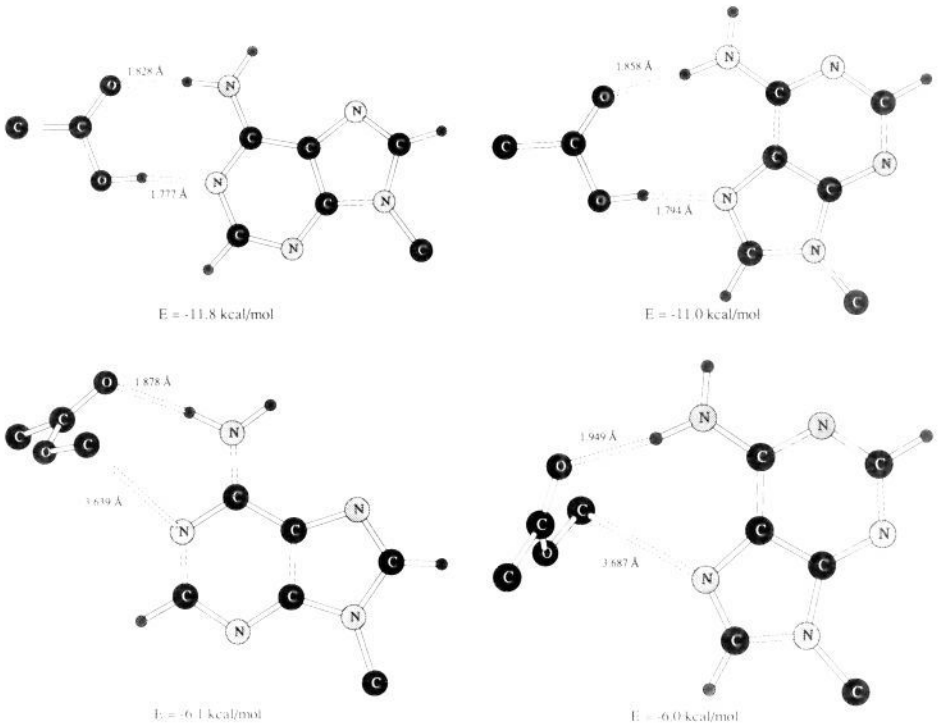

Figure 8. Optimized gas-phase structures of 9-Me-A with acetic acid and methyl acetate from the OPLS potential functions.

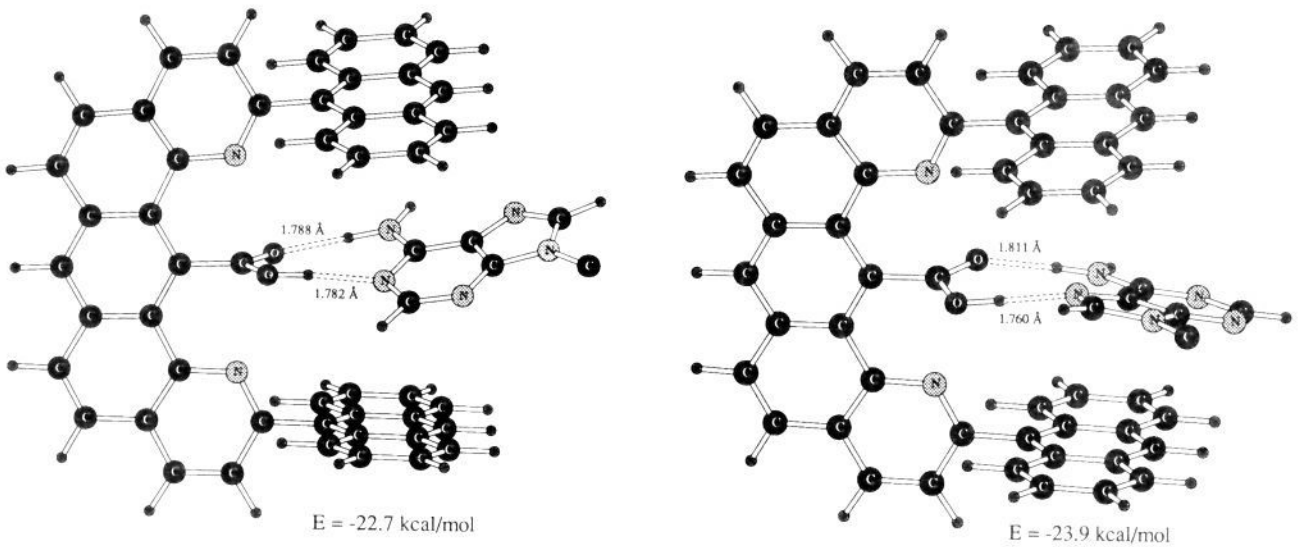

Figure 9. Comparison between Watson–Crick and Hoogsteen binding orientations obtained from gas-phase optimizations with the OPLS parameters for 9-Me-A with **6**.

Hoogsteen interactions corresponding to Figure 9 then actually strengthen a little to −24.4 and −25.2 kcal/mol. It is clear from these and other, extensive results[20,32] that attractive interactions for aromatic hydrocarbons or fragments are dominated by the Lennard-Jones (van der Waals) interactions. The contribution from the Coulomb interactions is comparatively minor and may even be somewhat repulsive as in the present case until the π-fragments and the guest have significant dipole moments. The insensitivity to the choice of charges does not carry over to hydrogen-bonding groups. If the AM1 charges are used for all atoms including the acid group in **6**, the optimal interaction energies with 9-Me-A become −18.1 and −19.3 kcal/mol in the Watson–Crick and Hoogsteen orientations. To guarantee correct thermodynamic and structural results for hydrogen-bonded liquids, it has been necessary to obtain the OPLS charges for hydrogen-bonding groups through iterative fitting with fluid simulations.[18,19]

(32) Williams, D. E. *Acta Crystallogr.* **1974**, *A30*, 71.

Conclusion

The present results have helped elucidate the adenine-binding characteristics of the molecular tweezers. For the acid tweezer **6**, the remarkably strong gas-phase interaction with 9-methyladenine was found to result roughly as much from π-stacking as the double hydrogen bonding. This clearly points out the potential of aromatic–aromatic interactions for molecular design that is also reflected in the host–guest chemistry of cyclophanes.[33] The strong binding of adenine derivatives by the acid tweezers in chloroform

(33) Diederich, F. *Angew. Chem., Int. Ed. Engl.* **1988**, *27*, 362.

(34) **Note added in proof**: Binding data in chloroform have recently been reported for two new acid tweezers (Zimmerman, S. C.; Zeng, Z. *J. Org. Chem.* **1990**, *55*, 4789). The tweezer corresponding to **3** with phenyl replacing dimethylanilinyl yields a free energy of binding, ΔG_b, of −5.7 kcal/mol with 9-propyladenine. In addition, the acid tweezer with the phenyl substituent and a fully unsaturated pentacyclic spacer has been prepared; it gives a ΔG_b of −6.9 kcal/mol with 9-propyladenine, which can be compared to the predicted value of −5.7 ± 0.6 kcal/mol for the desphenyl analogue **6** with 9-Me-A.

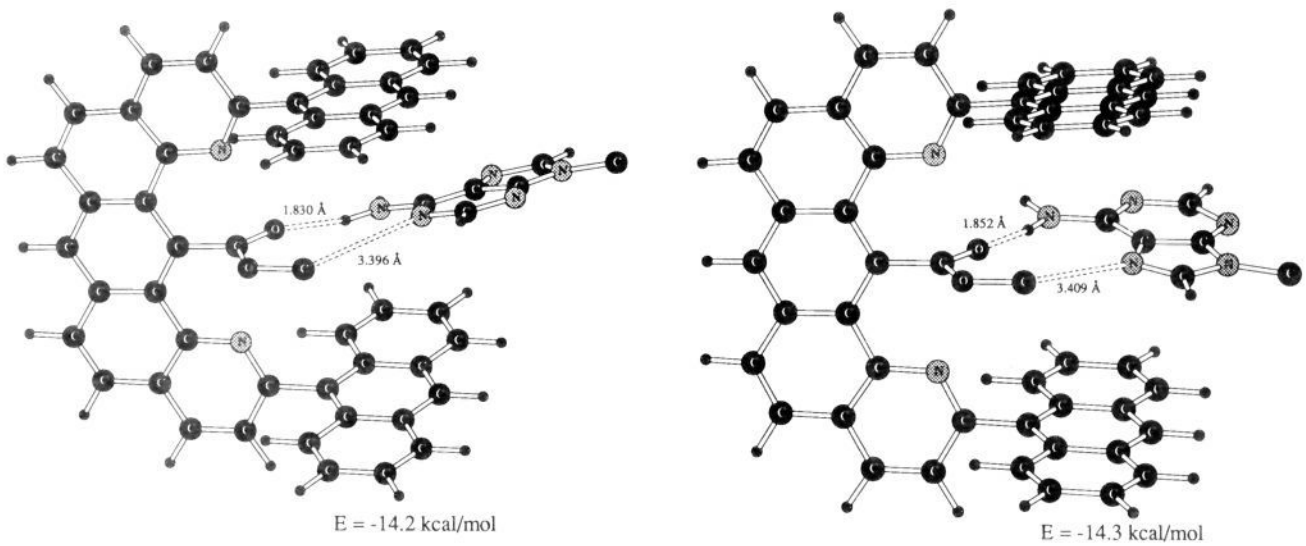

Figure 10. Comparison between Watson–Crick and Hoogsteen binding orientations obtained from gas-phase optimizations with the OPLS parameters for 9-Me-A with **7**.

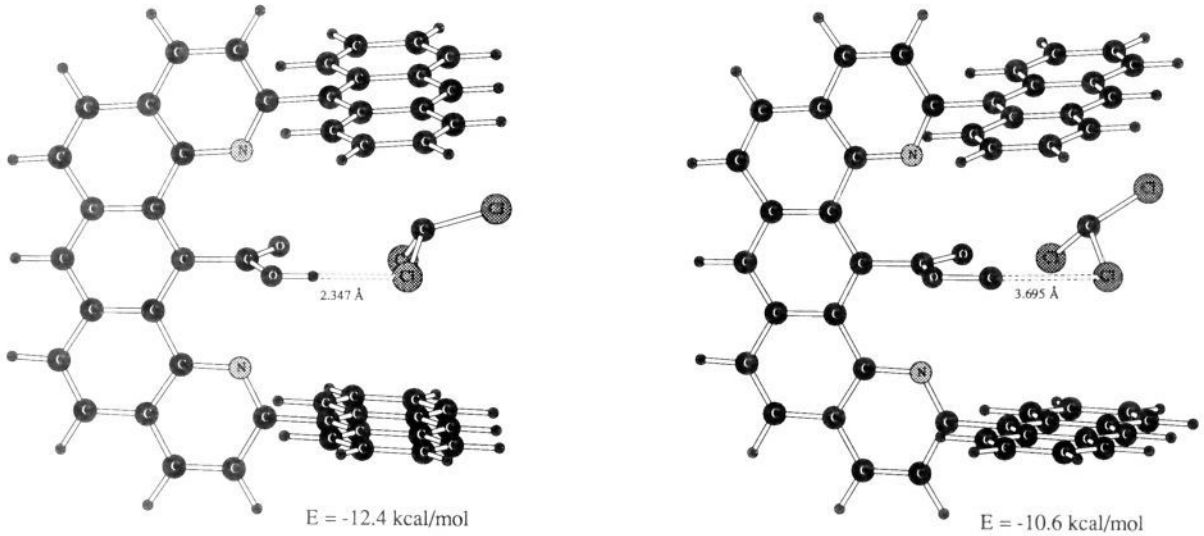

Figure 11. Optimized gas-phase complexes of chloroform with tweezers **6** and **7**. Note the hydrogen of chloroform is implicit in the OPLS four-site model.

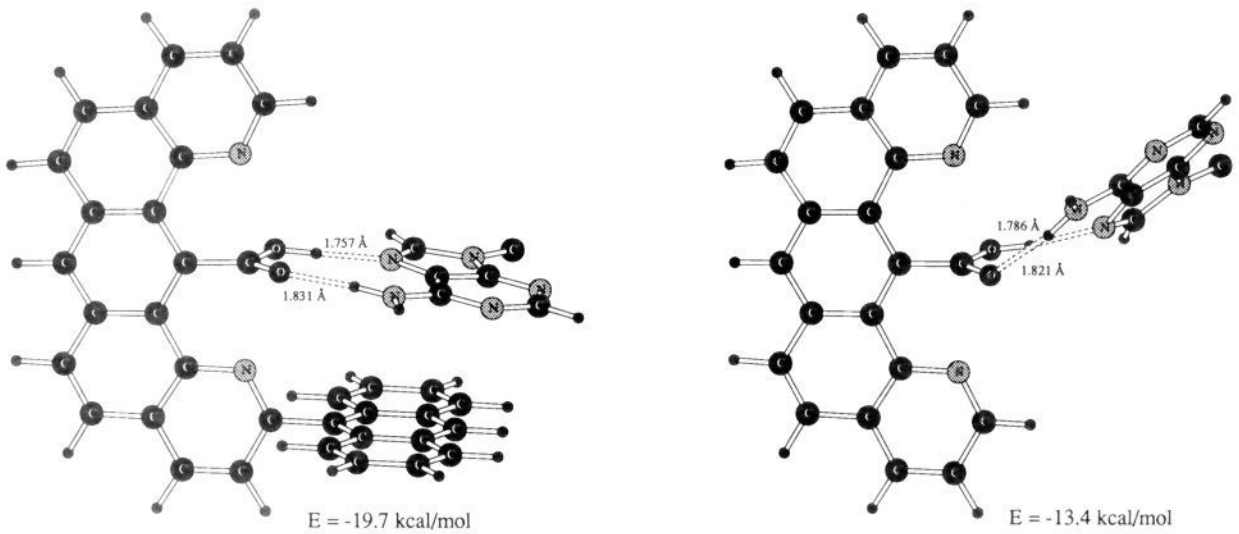

Figure 12. Optimized gas-phase structures of 9-Me-A with **6** following successive replacement of one and two anthracyl units with hydrogen.

was not found to be enhanced by a lack of solvation of the binding cleft. In fact, interactions between chloroform and the anthracene plates of the tweezers lead to strong binding of chloroform in the cleft. For the acid tweezer, the differential favoring binding 9-Me-A over chloroform is enough to enable the displacement of the solvent. However, the differential is not enough in the case of the ester tweezer to allow 9-Me-A to replace the one to two chloroform molecules in the cleft.

On the technical side, the present results have demonstrated the value of the double-annihilation route to computing absolute free energies of binding.[23] This is an important development for facilitating direct comparisons between theory and experiment in host-guest chemistry. The benefit for precision of using double-wide sampling[26] as opposed to performing all of the perturbations in one direction has also been documented. Care must still be exercised in keeping the perturbation steps small to avoid degradation of precision. As noted previously,[20] this concern is amplified in a more cohesive and structured solvent such as water in comparison to most organic solvents including chloroform. Though the computational effort is currently large, continuing enhancements in computational resources will make calculation of free energies of binding in solution routine.

Acknowledgment. Gratitude is expressed to the National Science Foundation for support of this research and to Professor Steven C. Zimmerman for helpful discussions and data before publication.

Supplementary Material Available: Complete specifications of the geometries of 9-methyladenine, **6**, and **7** in Z-matrix format (5 pages). Ordering information is given on any current masthead page.

Electron Transfer across Polypeptides. 6. Long-Range Electron Transfer in Osmium-Ruthenium Binuclear Complexes Bridged with Oligoproline Peptides

Asbed Vassilian,[†] James F. Wishart,[§] Bruno van Hemelryck,[†] Harold Schwarz,*[,§] and Stephan S. Isied*[,†]

Contribution from the Departments of Chemistry, Rutgers, The State University of New Jersey, New Brunswick, New Jersey 08903, and Brookhaven National Laboratory, Upton, New York 11973. *Received February 7, 1990*

Abstract: A series of binuclear $[(NH_3)_5Os(Pro)_nCo(NH_3)_5](CF_3COO)_5$ (n = 0-4) complexes have been synthesized. Long range intramolecular electron transfer reactions in these polypeptides were studied by the formation of the $Os^{II}(Pro)_n$isoRu^{III} precursor complexes by using reducing radicals (ca. CO_2^- and e_{aq}) generated by pulse radiolysis techniques. For the n = 0 complex, the intramolecular electron-transfer rate was very fast, and only a lower limit of 5×10^9 s^{-1} could be estimated at 25 °C. For the n = 1-3 complexes, the rates and activation parameters for electron transfer were determined to be 3.1×10^6 s^{-1}, $\Delta H^* = 4.2$ kcal/mol, $\Delta S^* = -15$ eu/mol; 3.7×10^4 s^{-1}, $\Delta H^* = 5.9$ kcal/mol, $\Delta S^* = -19$ eu/mol; 3.2×10^2 s^{-1}, $\Delta H^* = 7.4$ kcal/mol, and $\Delta S^* = -23$ eu/mol, respectively. For n = 4, only a rate constant of 50 s^{-1} at 25 °C was observed. By using a rearranged form of the transition-state expression, a plot of $\ln k + \Delta H^*/RT$ vs distance can be used to separate the electronic factor from the nuclear reorganization factor for these electron-transfer reactions. This analysis yielded a slope for the electronic factor $\beta = 0.65$ Å^{-1}. The results of the experiments presented here show that rapid rates of electron transfer across polypeptides can be observed for a metal-to-metal separation of >20 Å even for a low driving force for the reaction ($\Delta E° = 0.25$ eV). These results can be used to predict fast rates of electron transfer (ca. in the millisecond time scale) across metal-to-metal distances of 40 Å if the driving force and reorganization energy are appropriately controlled.

Introduction

Rates of electron-transfer (ET) reactions can vary by more than 18 orders of magnitude, ranging in time scale from subpicoseconds to many hours and days. Understanding the mechanism of these ET processes requires a detailed study of the factors that influence their rates.[1,2] These factors include distance, reorganization energy, driving force, and the electronic structure of the donor and acceptor as well as the bridging ligand that connects them. Recent studies have focused on *intra*molecular ET reactions where the electron-transfer step in a donor-acceptor complex occurs without complications from diffusion and other molecular interactions. In such molecules, systematic variations in the factors controlling the rates can be studied.

One of the important factors that control the rate of these reactions is the distance between the donor and the acceptor. In most cases studied, the rate of the intramolecular ET reactions was shown to decrease as the distance between the donor and acceptor increases; however, the magnitude of this decrease varied with the nature of the donor-acceptor molecules studied.[1-10] To investigate the effect of distance on intramolecular ET under controlled conditions, we and other groups have designed binuclear

[†] Rutgers University.
[§] Brookhaven National Laboratory.

(1) Isied, S. S. *Prog. Inorg. Chem.* **1984**, *32*, 443-557.
(2) (a) Marcus, R. A.; Sutin, N. *Biochim. Biophys. Acta* **1985**, *811*, 265. (b) Sutin, N.; Brunschwig, B.; Creutz, C.; Winkler, J. R. *Pure Appl. Chem.* **1988**, *60*, 1817. (c) Sutin, N. *Acc. Chem. Res.* **1982**, *15*, 275. (d) Sutin, N. In *Supramolecular Photochemistry*; Balzani, V., Ed.; Riedel: 1987; Proceedings of NATO Workshop, April 1987, Italy.
(3) (a) Isied, S. S.; Taube, H. *J. Am. Chem. Soc.* **1973**, *95*, 8198-8200. (b) Schaffer, L. J.; Taube, H. *J. Phys. Chem.* **1986**, *90*, 3669. (c) Rieder, K.; Taube, H. *J. Am. Chem. Soc.* **1977**, *99*, 7891. (d) Fischer, H.; Tom, G. M.; Taube, H. *J. Am. Chem. Soc.* **1976**, *98*, 5512.
(4) (a) Szecsy, A. P.; Haim, A. *J. Chem. Soc.* **1981**, *103*, 1679. (b) Haim, A. *Prog. Inorg. Chem.* **1983**, *30*, 273. (c) Haim, A. *Pure Appl. Chem.* **1983**, *55*, 89. (d) Lee, G.; Ciana, L.; Haim, A. *J. Am. Chem. Soc.* **1989**, *111*, 2535.
(5) Endicott, J. F. *Acc. Chem. Res.* **1988**, *21*, 59.
(6) (a) Warman, J. M.; de Haas, M. P.; Oevering, H.; Verhoeven, J. W.; Paddon-Row, M. N.; Oliver, A. M.; Hush, N. S. *Chem. Phys. Lett.* **1986**, *128*, 95. (b) Oevering, H.; Paddon-Row, M. N.; Heppener, M.; Oliver, A. M.; Cotsaris, E.; Verhoeven, J. W.; Hush, N. S. *J. Am. Chem. Soc.* **1987**, *109*, 3258. (c) Penfield, K. W.; Miller, J. R.; Paddon-Row, M. N.; Cotsaris, E.; Oliver, A. M.; Hush, N. S. *J. Am. Chem. Soc.* **1987**, *109*, 5061.
(7) (a) Wasielewski, M. R.; Niemczyk, M. P.; Svec, W. A.; Pewitt, E. B. *J. Am. Chem. Soc.* **1985**, *107*, 1080. (b) Wasielewski, M. R.; Niemczyk, M. P.; Pewitt, E. B. *J. Am. Chem. Soc.* **1985**, *107*, 5562.

0002-7863/90/1512-7278$02.50/0